AD-A095 079 DEFENCE RESEARCH ESTABLISHMENT VALCARTIER (QUEBEC) F/G 20/5
FOCUSED LASER BEAMS IN TURBULENT MEDIA,(U)
DEC 80 L R BISSONNETTE
UNCLASSIFIED DREV-R-4178/80 NL

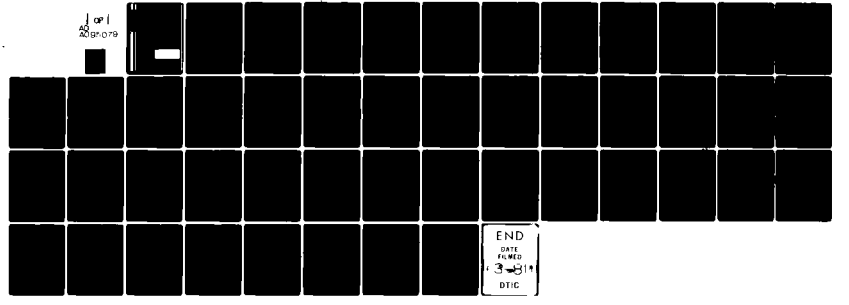

UNCLASSIFIED

UNLIMITED DISTRIBUTION
ILLIMITÉE

AD A095079

LEVEL II

DTIC
ELECTE
FEB 13 1981
E

FILE COPY

Centre de Recherches pour la Défense
Defence Research Establishment
Valcartier, Québec

BUREAU RECHERCHE ET DEVELOPPEMENT
MINISTERE DE LA DEFENSE NATIONALE
CANADA

RESEARCH AND DEVELOPMENT BRANCH
DEPARTMENT OF NATIONAL DEFENCE
CANADA

81 2 17 209

CRDV R-4178/80
DOSSIER: 3633B-007

UNCLASSIFIED

DREV-R-4178/80
FILE: 3633B-007

FOCUSED LASER BEAMS IN TURBULENT MEDIA

by

L.R. Bissonnette

CENTRE DE RECHERCHES POUR LA DEFENSE
DEFENCE RESEARCH ESTABLISHMENT
VALCARTIER
Tel: (418) 844-4271

Québec, Canada

December/décembre 1980

NON CLASSIFIE

RESUME

On dérive un système fermé de trois équations simultanées aux dérivées partielles pour résoudre l'intensité moyenne et la variance de l'intensité de faisceaux laser focalisés se propageant dans un milieu turbulent. Ces équations sont uniformément valides à tous les niveaux de scintillation. Des exemples de solutions calculées numériquement sont en excellent accord avec des mesures obtenues dans l'atmosphère et en laboratoire. On dérive de ces équations une expression analytique de la diffusion par la turbulence et on démontre que celle-ci est plus précise que la formule généralement employée et tirée du concept du diamètre de cohérence ρ_o. Dans la limite des scintillations faibles, la solution pour la variance de l'intensité recoupe les résultats classiques de la théorie de perturbation. (NC)

ABSTRACT

A closed set of three simultaneous partial differential equations is derived for the solution of the average irradiance and the irradiance variance of focused laser beams in a turbulent medium. The equations are uniformly valid for arbitrary scintillation levels. Examples of solutions calculated by finite difference techniques agree very well with experimental data in the atmosphere and in the laboratory. An analytic expression for the turbulence-induced beam spreading is obtained and shown to be more precise than the commonly used formula based on the coherence diameter ρ_o. In the weak scintillation limit, the irradiance variance solution agrees with the classical perturbation results. (U)

TABLE OF CONTENTS

1.0 INTRODUCTION

Atmospheric turbulence can seriously affect the propagation of a laser beam. The refractive index turbulence induces phase and amplitude fluctuations which cause the beam to scintillate or break up in several random patches, to lose its spatial coherence, to wander about its axis, and to spread out. Numerous analytical treatments of these phenomena have already been published. The analytical Rytov method, fully documented in Refs. 1 and 2, gives excellent results in the weak scintillation regime, i.e. at small propagation distance and/or turbulence strength. However, it is well-known that the Rytov method fails when irradiance fluctuations reach a certain level: theory predicts an unlimited increase of the irradiance variance whereas experiments definitely show saturation. Many recent models deal with this problem and predict, with variable degrees of accuracy, the phenomenon of saturation. A first approach, known as the renormalization technique, is described in Ref. 2. For example, it is used by De Wolf (Refs. 3-6) to predict the saturation of the irradiance variance. A second approach consists in solving the differential equation for the fourth-order statistical moment of the complex electric field closed by the local application of the method of small perturbations. This method is reviewed in Ref. 7 and examples of solutions showing saturation are given in Refs. 7-11. A third approach is based on the extension of the Huygens-Fresnel principle to turbulent media (Ref. 12). Saturation results derived from various applications of this principle may be found in Refs. 13-17.

The models listed in the preceding paragraph are generally well corroborated by measurements. However, they all require lengthy calculations to compute the average irradiance and the irradiance variance profiles of finite laser beams. One has either to solve a fourfold partial differential equation or to evaluate multiple integrals at each spatial point. In particular, these models are not suitable for the calculation of nonlinear propagation in the presence of turbulence,

such as thermal blooming. To fill this need, the present report proposes a calculation method of beam propagation in turbulence which is numerically simple, fast and uniformly applicable to arbitrary scintillation levels.

In Ref. 18, we developed a model in the form of linear, second-order partial differential equations for the first- and second-order moments of the complex wave amplitude. These equations can be easily solved numerically to calculate the average irradiance and the irradiance variance profiles of laser beams in turbulence. The approach is similar to that used in the calculation of turbulent shear flows (see for instance Chap. 5 of Ref. 19). The differential equations for the statistical moments of the complex wave amplitude are derived from the stochastic wave equation. Since the latter is quasi-linear owing to the nonhomogeneous refractive index, the resulting system of equations is unclosed. To resolve this difficulty, expressions are sought to relate the unknown or higher order moments to the first- and second-order complex-amplitude moments. In Ref. 18, these closure relations were derived from mostly empirical considerations but the accuracy of the resulting solutions was so consistent that it prompted us to investigate further into this approach.

The closure relations necessary to solve the average irradiance were rederived in Ref. 20 in a fully consistent manner from the governing wave equation. However, one empirically based relation is still needed to predict the higher order irradiance variance. The empirical input appears in the form of one universal complex constant. To eliminate this constant, we would have to consider the equation for the covariance of the complex amplitude and, thus, go back to the complexity of at least fourfold partial differential equations which we set out to avoid. Hence, we believe that the level of empiricism remaining in the model is acceptable and certainly well compensated for by the simplicity it affords.

The results of Ref. 20 are strictly applicable to collimated beams. In this report, we extend the model to include focalization. Section 2.0 is a short review of the theoretical background. Section 3.0 gives the closure relations. Section 4.0 compares solutions with data taken in a simulation experiment and in the atmosphere. Finally, section 5.0 presents simplified analytical solutions valid under practical operating conditions.

This work was performed at DREV between October 78 and November 79 under PCN 33B07, Atmospheric Propagation of Laser Beams.

2.0 THEORETICAL BACKGROUND

Our mathematical model for optical wave propagation is described in Refs. 18 and 20. In short, the scalar electric field E of a monochromatic wave propagating in the z direction under negligible polarization effects satisfies the equation

$$\underset{\sim}{\nabla}_3 E + \frac{k^2 N^2}{n_o^2} E = 0, \qquad [1]$$

where $\underset{\sim}{\nabla}_3$ is the three-dimensional gradient operator, $k = n_o\omega/c$ is the optical wave number, n_o is the unperturbed index of refraction, ω is the optical angular frequency of the source, c is the speed of light in free space, and N is the instantaneous random index of refraction. The electric field E is written as follows:

$$E = A \exp[ik(\phi+z) - i\omega t], \qquad [2]$$

where A and ϕ will be specified below. Upon substituting eq. 2 for E in eq. 1 and making the paraxial approximation valid for propagation in atmospheric turbulence, we obtain after separation

$$\left(\frac{\partial}{\partial z} + \underset{\sim}{V}\cdot\underset{\sim}{\nabla}\right)\underset{\sim}{V} = \underset{\sim}{\nabla}(N-n_o)/n_o, \qquad [3]$$

$$\left(\frac{\partial}{\partial z} + \underset{\sim}{V}\cdot\underset{\sim}{\nabla}\right)A + 1/2\ A\underset{\sim}{\nabla}\cdot\underset{\sim}{V} - \frac{i}{2k}\nabla^2 A = 0, \qquad [4]$$

where $\underset{\sim}{\nabla}$ is the gradient operator in the plane normal to the 0-z axis, and

$$\underset{\sim}{V} = \underset{\sim}{\nabla}\phi\ . \qquad [5]$$

In obtaining eq. 3, it was assumed that $(N-n_o)/n_o << 1$ which is well verified in atmospheric turbulence.

The separation into eqs. 3 and 4 is different from common practice. Consequently, functions A and ϕ differ from classical amplitude and phase. The advantage of this particular separation is that the equation for $\underset{\sim}{V}$ is independent of A. It is easy to verify that eq. 3 is the paraxial form of the eikonal equation of geometrical optics. Hence, the surfaces ϕ = constants are the geometrical-wave fronts and $\underset{\sim}{V}(z,\underset{\sim}{r})$ is the component, in the transverse plane, of the unit vector parallel to the geometrical ray passing through the point $(z,\underset{\sim}{r})$. $\underset{\sim}{V}(z,\underset{\sim}{r})$ can also be interpreted as the vector angle subtended by the ray at that

point and will be referred to as the angle-of-arrival. Finally, from eq. 2, it follows that A is the complex amplitude defined on the geometrical phase fronts. This complex amplitude embodies the diffractional phase.

Since the refractive index N is a random function, eqs. 3 and 4 are stochastic equations. There is no known general method of solving the random functions $\underset{\sim}{V}$ and A. Even if that could be achieved, it would yield much more information than required in practice. Here, the stochastic eqs. 3 and 4 are used to obtain the differential equations for the statistical moments of $\underset{\sim}{V}$ and A. We limit ourselves to the first- and second-order moments which lend themselves to straightforward physical interpretations.

The random functions are written as sums of an average and a fluctuating part, i.e.:

$$N = \langle N \rangle + n; \quad \langle n \rangle = 0, \qquad [6]$$

$$\underset{\sim}{V} = \langle \underset{\sim}{V} \rangle + \underset{\sim}{v}; \quad \langle \underset{\sim}{v} \rangle = 0, \qquad [7]$$

$$A = \langle A \rangle + a; \quad \langle a \rangle = 0, \qquad [8]$$

where the angular brackets denote ensemble averaging. The equations for the moments are obtained by taking the ensemble average of the stochastic equations for $\underset{\sim}{V}$, A, AA and AA* derived from the governing eqs. 3 and 4. We find:

$$\left(\frac{\partial}{\partial z} + \langle \underset{\sim}{V} \rangle \cdot \underset{\sim}{\nabla}\right) \langle \underset{\sim}{V} \rangle = - 1/2 \, \underset{\sim}{\nabla} \langle \underset{\sim}{v} \cdot \underset{\sim}{v} \rangle + \underset{\sim}{\nabla}(\langle N \rangle - n_o)/n_o \, , \qquad [9]$$

$$\left(\frac{\partial}{\partial z} + \langle \underset{\sim}{V} \rangle \cdot \underset{\sim}{\nabla}\right) \langle A \rangle + 1/2 \, \langle A \rangle \underset{\sim}{\nabla} \cdot \langle \underset{\sim}{V} \rangle - \frac{i}{2k} \nabla^2 \langle A \rangle = - \underset{\sim}{\nabla} \cdot \langle \underset{\sim}{v} a \rangle + 1/2 \langle a \underset{\sim}{\nabla} \cdot \underset{\sim}{v} \rangle \, , \qquad [10]$$

$$\left(\frac{\partial}{\partial z} + \langle \underset{\sim}{V} \rangle \cdot \underset{\sim}{\nabla}\right) \langle aa \rangle + \langle aa \rangle \underset{\sim}{\nabla} \cdot \langle \underset{\sim}{V} \rangle - \frac{i}{2k} \nabla^2 \langle aa \rangle + \frac{i}{k} \langle \underset{\sim}{\nabla} a \cdot \underset{\sim}{\nabla} a \rangle$$

$$= - \underset{\sim}{\nabla} \cdot \langle \underset{\sim}{v} aa \rangle - 2 \langle a \underset{\sim}{v} \rangle \cdot \underset{\sim}{\nabla} \langle A \rangle - \langle A \rangle \langle a \underset{\sim}{\nabla} \cdot \underset{\sim}{v} \rangle \, , \qquad [11]$$

$$\left(\frac{\partial}{\partial z} + \langle \underset{\sim}{V} \rangle \cdot \underset{\sim}{\nabla}\right) \langle aa^* \rangle + \langle aa^* \rangle \underset{\sim}{\nabla} \cdot \langle \underset{\sim}{V} \rangle - \frac{i}{2k} \left[\langle a^* \nabla^2 a \rangle - \langle a \nabla^2 a^* \rangle \right]$$

$$= - \underset{\sim}{\nabla} \cdot \langle \underset{\sim}{v} aa^* \rangle - \langle a \underset{\sim}{v} \rangle \cdot \underset{\sim}{\nabla} \langle A \rangle^* - \langle a^* \underset{\sim}{v} \rangle \cdot \underset{\sim}{\nabla} \langle A \rangle \qquad [12]$$

$$- 1/2 \, \langle A \rangle^* \langle a \underset{\sim}{\nabla} \cdot \underset{\sim}{v} \rangle - 1/2 \, \langle A \rangle \langle a^* \underset{\sim}{\nabla} \cdot \underset{\sim}{v} \rangle \, ,$$

where the superscript * denotes a complex conjugate.

The system of eqs. 10-12 for $\langle A \rangle$, $\langle aa \rangle$ and $\langle aa^* \rangle$ is mathematically unclosed insofar as it contains more unknowns than equations, namely the moments $\langle \underset{\sim}{v} a \rangle$, $\langle \underset{\sim}{v} aa \rangle$, $\langle \underset{\sim}{v} aa^* \rangle$ and $\langle a \underset{\sim}{\nabla} \cdot \underset{\sim}{v} \rangle$. In principle, one could derive equations for these moments using a procedure analogous to that used in obtaining eqs. 10-12. However, one would quickly realize that this technique leads to equations involving still higher

order and unknown moments. This is the classical closure problem which is always encountered in the treatment of statistical phenomena governed by nonlinear and/or quasi-linear stochastic equations such as eqs. 3 and 4. Of course, there is no exact method of solution for this problem since the complete mathematical model contains an infinite number of equations. Hence, workable models require closing the hierarchy of equations after moments of a given order. This can be accomplished only through approximations regarding the higher order moments for which the equations have been left out. In this paper, we derive four relations to express $\langle \underset{\sim}{\nu} a \rangle$, $\langle \underset{\sim}{\nu} aa \rangle$, $\langle \underset{\sim}{\nu} aa^* \rangle$ and $\langle a \underset{\sim}{\nabla} \cdot \underset{\sim}{\nu} \rangle$ as functions of $\langle A \rangle$, $\langle aa \rangle$ and $\langle aa^* \rangle$.

3.0 CLOSURE RELATIONS

The derivation of the closure relations is based on three principal hypotheses.

I. The fluctuating angle-of-arrival $\underset{\sim}{\nu}$ is statistically homogeneous and isotropic in the plane transverse to the 0-z axis. This approximation follows from the hypothesis that the refractive index is statistically homogeneous and isotropic and from the paraxial approximation. Indeed, since the medium is homogeneous and isotropic and since the average ray angle $\langle \underset{\sim}{V} \rangle$ is small, the rays reaching a plane z traverse statistically equivalent paths. Hence, the covariance function of $\underset{\sim}{\nu}$ should depend only on the relative positions of the observation points in plane z.

II. The random complex amplitude and angle-of-arrival are only weakly correlated. This approximation is based on the observation that the fluctuating complex amplitude $a(z,\underset{\sim}{r})$ is the result of repeated interactions with the angle-of-arrival over the complete propagation path between 0 and z. Hence, $a(z,\underset{\sim}{r})$ depends on many processes independent of the local angle-of-arrival $\underset{\sim}{\nu}(z,\underset{\sim}{r})$. Moreover, eq. 3 shows that

$\underset{\sim}{v}$ is independent of "a". Therefore, the hypothesis of weak correlation appears very plausible. More specifically, we assume

$$\langle \underset{\sim}{v}_1 a_2 \rangle \ll \langle \underset{\sim}{v}\cdot\underset{\sim}{v} \rangle^{1/2} \langle I \rangle^{1/2} , \quad [13a]$$

$$\langle \underset{\sim}{v}_1 \underset{\sim}{v}_2 a_2 \rangle \ll \langle \underset{\sim}{v}\cdot\underset{\sim}{v} \rangle \langle I \rangle^{1/2} , \quad [13b]$$

$$\langle \underset{\sim}{v}_1 \underset{\sim}{v}_2 a_1 a_2 \rangle \approx \langle \underset{\sim}{v}_1 \underset{\sim}{v}_2 \rangle \langle a_1 a_2 \rangle + \{ |\text{terms}| \ll \langle \underset{\sim}{v}\cdot\underset{\sim}{v} \rangle \langle I \rangle \} , \quad [13c]$$

etc...,

where $\langle I \rangle = \langle A \rangle \langle A \rangle^* + \langle aa^* \rangle$ is the average irradiance. The subscripts 1 and 2 refer to the separation points of the covariance functions; where no subscripts are used, the midpoint between 1 and 2 is taken.

III. The covariance functions involving the fluctuating complex amplitude are quasi-homogeneous and quasi-isotropic in the transverse plane. More specifically, we set

$$\langle a(z_1, \underset{\sim}{r}_1) a(z_2, \underset{\sim}{r}_2) \rangle = F_{aa}\left(z_1, z_2; \frac{\underset{\sim}{r}_1 + \underset{\sim}{r}_2}{2}\right) g_{aa}(z_1, z_2; |\underset{\sim}{r}_1 - \underset{\sim}{r}_2|) , \quad [14a]$$

$$\langle a(z_1, \underset{\sim}{r}_1)a^*(z_2,\underset{\sim}{r}_2)\rangle = F_{aa^*}(z_1 z_2; \frac{\underset{\sim}{r}_1+\underset{\sim}{r}_2}{2})\ g_{aa^*}(z_1,z_2;|\underset{\sim}{r}_1-\underset{\sim}{r}_2|). \qquad [14b]$$

Under hypothesis I, eq. 9 becomes

$$\frac{\partial}{\partial z}\langle\underset{\sim}{V}\rangle + \langle\underset{\sim}{V}\rangle\cdot\underset{\sim}{\nabla}\langle\underset{\sim}{V}\rangle = \underset{\sim}{\nabla}(\langle N\rangle - n_o)/n_o, \qquad [15]$$

which shows that the average ray angle $\langle\underset{\sim}{V}\rangle$ is independent of the turbulent fluctuations. The solution of eq. 15 for an initially spherical phase front with radius of curvature F in a statistically homogeneous medium, i.e. $\langle N\rangle$ = constant, is given by

$$\langle\underset{\sim}{V}\rangle = \underset{\sim}{r}/(z-F). \qquad [16]$$

The equation for the fluctuating complex amplitude is obtained by subtracting eq. 10 from eq. 4. We find, using eq. 16

$$\frac{\partial}{\partial z}a + \frac{\underset{\sim}{r}}{(z-F)}\cdot\underset{\sim}{\nabla}a + \frac{a}{(z-F)} - \frac{i}{2k}\nabla^2 a = g(z,\underset{\sim}{r}), \qquad [17]$$

where

$$g(z,\underset{\sim}{r}) = -\underset{\sim}{v}\cdot\underset{\sim}{\nabla}\langle A\rangle - \frac{\langle A\rangle\nabla\cdot\underset{\sim}{v}}{2} - \underset{\sim}{\nabla}\cdot[\underset{\sim}{v}a - \langle\underset{\sim}{v}a\rangle] + 1/2[a\underset{\sim}{\nabla}\cdot\underset{\sim}{v} - \langle a\underset{\sim}{\nabla}\cdot\underset{\sim}{v}\rangle]\ . \qquad [18]$$

An implicit solution to eq. 17 with the boundary condition

$$a(0,\underset{\sim}{r}) = \lim_{|\underset{\sim}{r}|\to\infty} a(z,\underset{\sim}{r}) = 0, \qquad [19]$$

is given by

$$a(z,\underset{\sim}{r}) = L(z,\underset{\sim}{r};\, u,\underset{\sim}{s})\; g(u,\underset{\sim}{s}), \qquad [20]$$

where $L(z,\underset{\sim}{r};\, u,\underset{\sim}{s})$ is an integral operator defined as follows:†

$$L(z,\underset{\sim}{r};u,\underset{\sim}{s})g(u,\underset{\sim}{s}) = \frac{ik}{2\pi}\int_0^z \frac{du}{(u-z)} \iint_{-\infty}^{\infty} d^2s\; g(u,\underset{\sim}{s}) \exp\left\{\frac{ik}{2(z-u)}\frac{F-z}{F-u}\left|\frac{F-u}{F-z}\,\underset{\sim}{r}-\underset{\sim}{s}\right|^2\right\}. \qquad [21]$$

The closure relations for $\langle\underset{\sim}{\gamma}a\rangle$, $\langle a\underset{\sim}{\nabla}\cdot\underset{\sim}{\gamma}\rangle$, $\langle\underset{\sim}{\gamma}aa\rangle$ and $\langle\underset{\sim}{\gamma}aa^*\rangle$ are derived by first multiplying eq. 20 by $\underset{\sim}{\gamma}$, $\underset{\sim}{\nabla}\cdot\underset{\sim}{\gamma}$, $\underset{\sim}{\gamma}a$ and $\underset{\sim}{\gamma}a^*$ respectively and then taking the ensemble average. Hypotheses I, II and III are used to simplify the statistical moments of the form $\langle\underset{\sim}{\gamma}(z,\underset{\sim}{r})\; g(u,\underset{\sim}{s})\rangle$ which are operated on by $L(z,\underset{\sim}{r};u,\underset{\sim}{s})$. The details can be found in Refs. 18 and 20. We simply recall the results here. They are

$$\langle a\underset{\sim}{\nabla}\cdot\underset{\sim}{\gamma}\rangle = -\,K\,\langle A\rangle, \qquad [22]$$

†There is an error in the definition of the operator L in Ref. 20. The error concerns the effect of the curvature F and disappears in the limit of collimated beams. Since the solutions of Ref. 20 were calculated in that limit, the error does not affect the results and conclusions.

$$\langle \underset{\sim}{v}a \rangle = - \underset{\approx}{R} \cdot \underset{\sim}{\nabla} \langle A \rangle , \qquad [23]$$

$$\langle \underset{\sim}{v}aa \rangle = - 1/2 \, \underset{\approx}{P} \cdot \underset{\sim}{\nabla} \langle aa \rangle , \qquad [24]$$

$$\langle \underset{\sim}{v}aa^* \rangle = - 1/2 \, \underset{\approx}{Q} \cdot \underset{\sim}{\nabla} \langle aa^* \rangle , \qquad [25]$$

where

$$K = 1/2 \, L(z,\underset{\sim}{r};u,\underset{\sim}{s}) \, \underset{\sim}{\nabla}_r \underset{\sim}{\nabla}_s : \langle \underset{\sim}{v}(z,\underset{\sim}{r}) \underset{\sim}{v}(u,\underset{\sim}{s}) \rangle , \qquad [26]$$

$$\underset{\approx}{R} = L(z,\underset{\sim}{r};\, u,\underset{\sim}{s}) \, \langle \underset{\sim}{v}(z,\underset{\sim}{r}) \underset{\sim}{v}(u,\underset{\sim}{s}) \rangle , \qquad [27]$$

$$\underset{\approx}{P} = \underset{\approx}{R} , \qquad [28]$$

$$\underset{\approx}{Q} = \text{Real} \, \{\underset{\approx}{R}\} . \qquad [29]$$

Equations 22-25 form the basis of our model, they relate the higher order unknown moments to the lower order moments and, thus, close the system of equations for <A>, <aa> and <aa*>. The functional relationships described by eqs. 22-25 are consistent with the physical interpretation of the terms they model. The moment $\langle a\underset{\sim}{\nabla} \cdot v \rangle$ which causes the decay of the coherent amplitude <A> is proportional to <A>, and, therefore, it survives for plane and spherical waves as indeed it should.

But, the terms $\langle \underset{\sim}{\nu} a \rangle$, $\langle \underset{\sim}{\nu} aa \rangle$ and $\langle \underset{\sim}{\nu} aa^* \rangle$, responsible for beam spreading, are all proportional to gradients of the lower order mean-field quantities and, as expected, they vanish for plane and spherical waves. It is noteworthy that these relations are analogous with expressions successfully used to model the turbulent momentum, heat and mass transport terms in turbulent shear flows (see for example Chap. 1, 5 and 6 of Ref. 19). However, they were not simply hypothesized here, they were derived in a fully consistent manner from the governing stochastic wave equation.

Equations 26-29 show that the proportionality functions K, $\underset{\approx}{R}$, $\underset{\approx}{P}$ and $\underset{\approx}{Q}$ are all integrals of the covariance of the angle-of-arrival $\langle \underset{\sim}{\nu}(z,\underset{\sim}{r})\underset{\sim}{\nu}(u,\underset{\sim}{s}) \rangle$. An equation for $\underset{\sim}{\nu}$ is obtained by subtracting eq. 15 from eq. 3, i.e.

$$\frac{\partial}{\partial z}\underset{\sim}{\nu} + \langle \underset{\sim}{\nu} \rangle \cdot \underset{\sim}{\nabla}\underset{\sim}{\nu} + \underset{\sim}{\nu} \cdot \underset{\sim}{\nabla} \langle \underset{\sim}{\nu} \rangle + \underset{\sim}{\nu} \cdot \underset{\sim}{\nabla}\underset{\sim}{\nu} = \underset{\sim}{\nabla} n/n_o \, . \qquad [30]$$

Neglecting the nonlinear stochastic term $\underset{\sim}{\nu} \cdot \underset{\sim}{\nabla}\underset{\sim}{\nu}$, which is valid for propagation in turbulence since the fluctuating ray angle $|\underset{\sim}{\nu}|$ remains small throughout the propagation range, and using eq. 16 for $\langle \underset{\sim}{\nu} \rangle$, we have

$$\frac{\partial}{\partial z}\underset{\sim}{\nu} + \frac{\underset{\sim}{r}}{(z-F)} \cdot \underset{\sim}{\nabla}\underset{\sim}{\nu} + \frac{\underset{\sim}{\nu}}{(z-F)} = \underset{\sim}{\nabla} n/n_o . \qquad [31]$$

Solving along the average geometrical ray that passes through the point $(z,\underset{\sim}{r})$ and assuming that the path length along the ray can be approximated by z in accordance with the paraxial approximation, we find

$$\underset{\sim}{\nu}(z,\underset{\sim}{r}) \simeq \int_0^z d\zeta \, \frac{(\zeta-F)}{(z-F)} \, \frac{1}{n_o} \, \underset{\sim}{\nabla} n\left[\zeta, \, \underset{\sim}{r}' = \frac{F-\zeta}{F-z} \, \underset{\sim}{r}\right] . \qquad [32]$$

Therefore, the covariance of $\underset{\sim}{\nu}$ is given by:

$$\langle \underset{\sim}{\nu}(z,\underset{\sim}{r}) \underset{\sim}{\nu}(u,\underset{\sim}{s}) \rangle \simeq \frac{1}{n_o^2} \int_0^z d\zeta \int_0^u d\xi \, \frac{(\zeta-F)}{(z-F)} \, \frac{(\xi-F)}{(u-F)}$$
$$\cdot \underset{\sim}{\nabla}_{r'} \underset{\sim}{\nabla}_{r''} \left\langle n\left[\zeta, \, \underset{\sim}{r}' = \frac{F-\zeta}{F-z} \, \underset{\sim}{r}\right] \, n\left[\xi, \, \underset{\sim}{r}'' = \frac{F-\xi}{F-u} \, \underset{\sim}{s}\right] \right\rangle . \qquad [33]$$

Since the correlation scale of the index covariance function is much smaller than the propagation distances of interest, eq. 33 can be further approximated as follows:

$$\langle \underset{\sim}{\nu}(z,\underset{\sim}{r}) \underset{\sim}{\nu}(u,\underset{\sim}{s}) \rangle \simeq \frac{1}{n_o^2} \int_0^u d\zeta \, \frac{(\zeta-F)^2}{(z-F)(u-F)}$$
$$\cdot \underset{\sim}{\nabla}_{r'} \underset{\sim}{\nabla}_{r''} \int_{-\infty}^{\infty} d\tau \left\langle n[\zeta+\tau, \, \underset{\sim}{r}' = \underset{\sim}{r}''+\underset{\sim}{\Delta}] \, n\left[\zeta, \underset{\sim}{r}'' = \frac{F-\zeta}{F-u} \, \underset{\sim}{s}\right] \right\rangle . \qquad [34]$$

The vectors $\underset{\sim}{r}'$, $\underset{\sim}{r}''$ and $\underset{\sim}{\Delta}$ are defined in Fig. 1 which illustrates the geometrical features associated with the definition of the covariance function of $\underset{\sim}{\nu}$. In the paraxial approximation, the vector $\underset{\sim}{\Delta}$ is given by

$$\underset{\sim}{\Delta} \simeq \frac{F-\zeta}{F-z} \, \underset{\sim}{r} - \frac{F-\zeta}{F-u} \, \underset{\sim}{s} . \qquad [35]$$

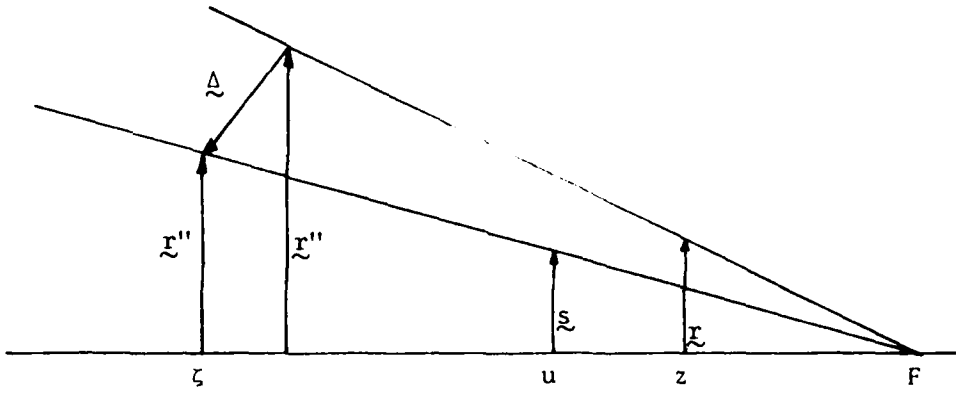

FIGURE 1 - Configuration of the rays and geometrical definition of the symbols for the calculation of the covariance function $\langle \chi(z,\underset{\sim}{r})\chi(u,\underset{\sim}{s})\rangle$.

The integral over τ has been worked out for homogeneous and isotropic Kolmogorov turbulence (Refs. 1 and 2). The result for eq. 34 is

$$\langle \chi(z,\underset{\sim}{r})\chi(u,\underset{\sim}{s})\rangle = \begin{cases} \displaystyle\int_o^u d\zeta \, \frac{(\zeta-F)^2}{(z-F)(u-F)} \, \frac{3.44\, C_n^2}{n_o^2\, \ell_o^{1/3}} \left[\underset{\sim}{a}_\Delta \underset{\sim}{a}_\Delta + \underset{\sim}{a}_\phi \underset{\sim}{a}_\phi\right]; \quad \Delta << \ell_o, \\ \displaystyle\int_o^u d\zeta \, \frac{(\zeta-F)^2}{(z-F)(u-F)} \, \frac{1.62\, C_n^2}{n_o^2\, \Delta^{1/3}} \left[\underset{\sim}{a}_\Delta \underset{\sim}{a}_\Delta + \frac{3}{2} \underset{\sim}{a}_\phi \underset{\sim}{a}_\phi\right]; \quad \Delta >> \ell_o, \end{cases} \qquad [36]$$

where C_n is the well-known structure constant of the turbulent refractive index and ℓ_o is the inner scale of turbulence. To simplify the algebra, we propose the following simple expression connecting the two asymptotic formula of eq. 36:

$$\langle \chi(z,\underset{\sim}{r})\chi(u,\underset{\sim}{s})\rangle = \frac{2.43\, C_n^2}{n_o^2} \int_o^u d\zeta \, \frac{(\zeta-F)^2}{(z-F)(u-F)} \, \frac{1}{\left[\Delta^2 + (.35\ell_o)^2\right]^{1/6}}$$

$$\cdot \left\{ \left[\underset{\sim}{a}_\Delta \underset{\sim}{a}_\Delta + \underset{\sim}{a}_\phi \underset{\sim}{a}_\phi\right] - \frac{1}{3} \, \frac{\Delta^2}{\left[\Delta^2 + (.35\, \ell_o)^2\right]} \, \underset{\sim}{a}_\Delta \underset{\sim}{a}_\Delta \right\}. \qquad [37]$$

Before substituting eq. 37 for the covariance of $\underset{\sim}{v}$ in eqs. 26 and 27 for the proportionality functions K and $\underset{\approx}{R}$, it is essential to match the geometry associated with eq. 37 to that associated with the definition of the operator L. This is best explained with reference to Fig. 2. The operator L was derived exactly and thus applies to spherical phase fronts. In particular, the argument of the exponential in eq. 21 is the phase difference between wavelets originating at A and B and arriving at P, i.e.

$$\Delta\phi_1 \simeq k\,[\overline{CD} - \overline{CB}]\,. \qquad [38]$$

Since all angles are small as required by the paraxial approximation, we have

$$\overline{CD} \simeq \frac{\overline{AC}^2}{2(z-u)}\,, \qquad [39]$$

$$\overline{CB} \simeq \frac{\overline{AC}^2}{2(F-u)}\,, \qquad [40]$$

$$\overline{AC}^2 \simeq \left|\frac{F-u}{F-z}\,\underset{\sim}{r} - \underset{\sim}{s}\right|^2\,. \qquad [41]$$

Hence, from eqs. 38-40 it follows that

$$\Delta\phi_1 = \frac{k}{2(z-u)}\,\frac{F-z}{F-u}\left|\frac{F-u}{F-z}\,\underset{\sim}{r} - \underset{\sim}{s}\right|^2\,, \qquad [42]$$

which is identical to the expression in eq. 21. However, as shown in Fig. 1, the geometry used to derive the covariance of $\underset{\sim}{y}$ is such that the transverse coordinate is not taken along circular arcs centered at z = F but rather along lines normal to the ray passing through $(z,\underset{\sim}{r})$. Thus, the argument of the exponential in eq. 21 should be replaced by the phase difference between the wavelets originating at A and C respectively and arriving at P, plus the phase difference between the spherical wave fronts passing through points A and C, i.e.

$$\Delta\phi_2 = k\,\overline{CD} + k\,\overline{CB} \qquad [43]$$

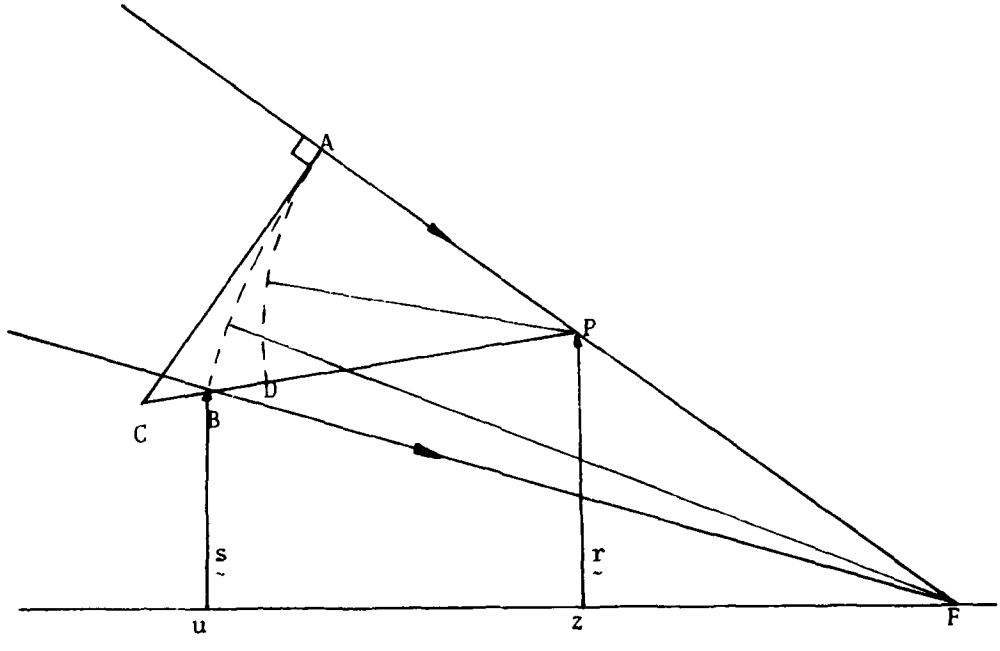

FIGURE 2 - Configuration of the rays and geometrical definition of the symbols for the calculation of the modified operator $L(z,\underset{\sim}{r};u,\underset{\sim}{s})$

Hence, from eqs. 39-41 and 43, we find

$$\Delta\phi_2 = \frac{k}{2(z-u)} \frac{F+z-2u}{F-u} \left| \frac{F-u}{F-z} \underset{\sim}{r} - \underset{\sim}{s} \right|^2 . \qquad [44]$$

Therefore, eqs. 26 and 27 are slightly modified as follows:

$$K = \frac{ik}{4\pi} \int_0^z \frac{du}{(u-z)} \iint_{-\infty}^{\infty} d^2s \; \underset{\sim}{\nabla}_r \underset{\sim}{\nabla}_s : \langle \underset{\sim}{v}(z,\underset{\sim}{r}) \underset{\sim}{v}(u,\underset{\sim}{s}) \rangle$$

$$\cdot \exp\left\{ \frac{ik}{2(z-u)} \frac{F+z-2u}{(F-\zeta)^2} \Delta^2 \right\} , \qquad [45]$$

$$R = \frac{ik}{2\pi} \int_0^z \frac{du}{(u-z)} \iint_{-\infty}^{\infty} d^2s \; \langle \underset{\sim}{v}(z,\underset{\sim}{r}) \underset{\sim}{v}(u,\underset{\sim}{s}) \rangle$$

$$\cdot \exp\left\{ \frac{ik}{2(z-u)} \frac{F+z-2u}{(F-\zeta)^2} \Delta^2 \right\} . \qquad [46]$$

Equation 37 shows that the covariance of $\underset{\sim}{v}$ is function of Δ^2 alone in the transverse plane. Since the integral operator in eqs. 45 and 46 is also dependent on Δ^2 alone, the resulting proportionality functions K and R depend on propagation distance z only.

Equation 37 is substituted for the covariance of $\underset{\sim}{\nu}$ in eqs. 45 and 46. The integration over the transverse plane can be performed analytically to give

$$K(z) = \frac{3.24\ C_n^2}{n_o^2\ \ell_1^{7/3}} \int_o^z du \int_o^u d\zeta\ \frac{(F-\zeta)^2 G(\gamma)}{(F-z)(F+z-2u)}\ , \qquad [47]$$

$$\underset{\approx}{R}(z) = \frac{2.43\ C_n^2}{n_o^2\ \ell_1^{1/3}}\ \underset{\approx}{\delta} \int_o^z du \int_o^u d\zeta\ \frac{(F-\zeta)^2\ H(\gamma)}{(F-z)(F+z-2u)}\ , \qquad [48]$$

where

$$G(\gamma) = (-i\gamma)^2 \left\{ \frac{1}{2} - 3i\gamma + [5/12 + i\gamma + 3\gamma^2] \frac{e^{-i\gamma}}{(-i\gamma)^{5/6}}\ \Gamma(5/6, -i\gamma) \right\}, \qquad [49]$$

$$H(\gamma) = (-i\gamma) \left\{ 1 + [5/6 + i\gamma]\ \frac{e^{-i\gamma}}{(-i\gamma)^{5/6}}\ \Gamma(5/6, -i\gamma) \right\}, \qquad [50]$$

$$\gamma = \frac{k\ell_1^2}{2(z-u)}\ \frac{(F+z-2u)(F-u)}{(F-\zeta)^2}\ , \qquad [51]$$

and where $\ell_1 = 0.35\ \ell_o$, $\underset{\approx}{\delta}$ is the unit dyad and $\Gamma(5/6, -i\gamma)$ is an incomplete Gamma function as defined by formula 6.5.20 of Ref. 21. The functions $G(\gamma)$ and $H(\gamma)$ are plotted in Figs. 3 and 4 respectively.

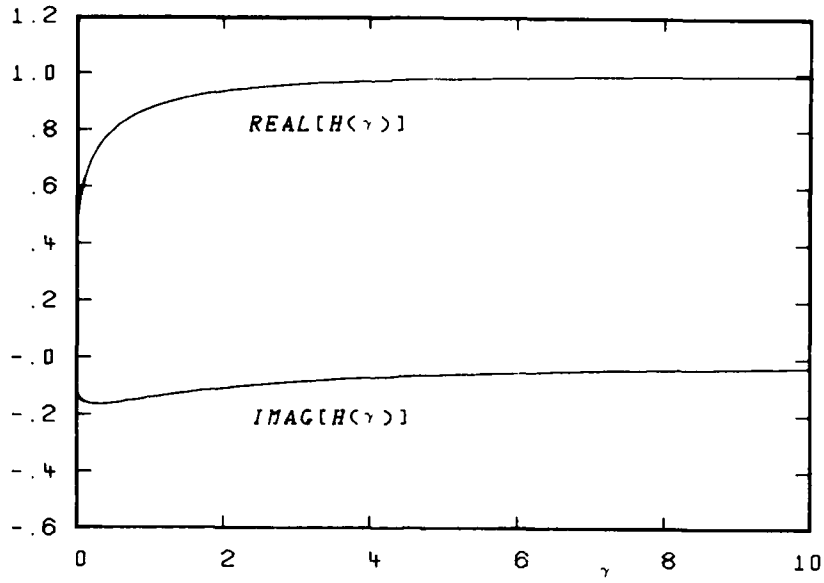

(a)

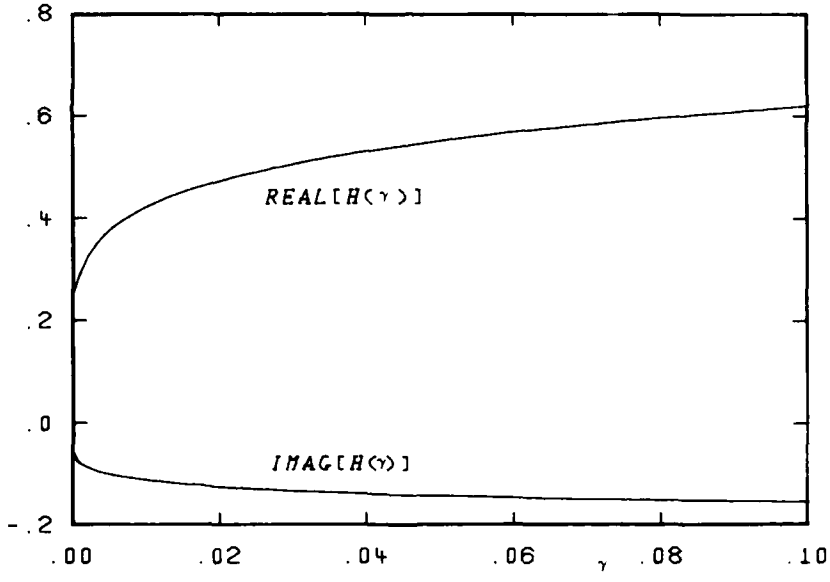

(b)

FIGURE 3 - Graph of the function H(γ)

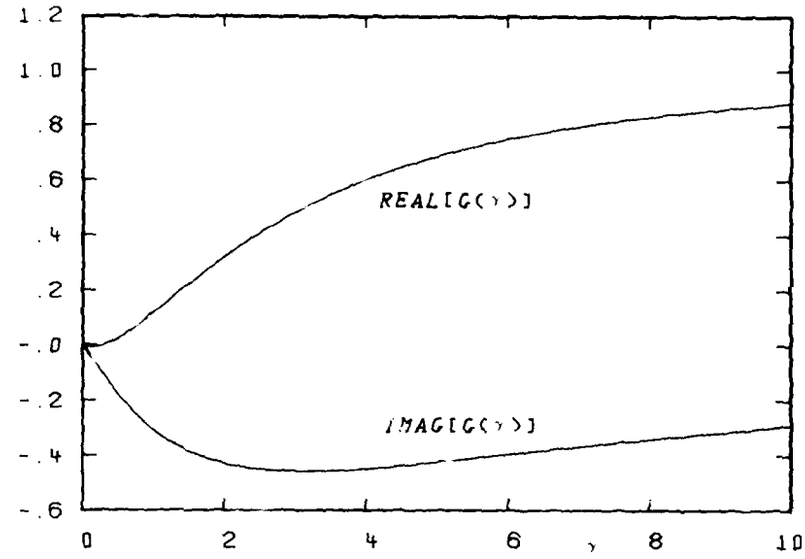

(a)

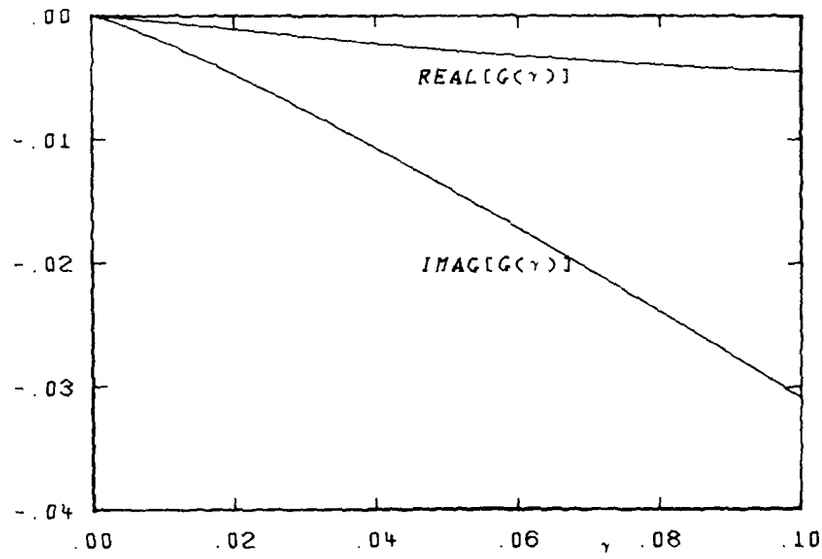

(b)

FIGURE 4 - Graph of the function G(γ)

The closure eqs. 22-25 together with the eqs. 47 and 48 for the proportionality functions K(z) and R(z) are sufficient to solve for the average irradiance. However, to calculate the irradiance variance profiles, we need a relation for the moment $\langle \underset{\sim}{\nabla} a \cdot \underset{\sim}{\nabla} a \rangle$. The latter was derived in a semi-empirical fashion in Ref. 20. As mentioned in the introduction, a more theoretical treatment of $\langle \underset{\sim}{\nabla} a \cdot \underset{\sim}{\nabla} a \rangle$ would require solving for the covariance function of the amplitude, hence recourse to multidimensional partial differential equations. This is beyond the scope of the present report and, therefore, the result of Ref. 20 multiplied by a geometrical factor to account for focalization will be simply taken here, i.e.

$$\langle \underset{\sim}{\nabla} a \cdot \underset{\sim}{\nabla} a \rangle - \frac{1}{4} \nabla^2 \langle aa \rangle = \begin{cases} C \dfrac{F-z/2}{F-z} \dfrac{k}{z} \langle aa \rangle; & z \leq z_A , \\ C \dfrac{F-z/2}{F-z} \dfrac{kz}{z_A^2} \langle aa \rangle; & z > z_A , \end{cases} \qquad [52]$$

where C is a universal empirical constant whose best rounded value is C=0.5-0.01 i† and z_A is a length scale defined in the next section. Finally, by virtue of the approximation of quasi-homogeneity and quasi-isotropy, i.e. eq. 14b, and from standard diffraction results, we have

---

† In Refs. 18 and 20, the constant was chosen equal to 0.3 - 0.01 i. The effect on the resulting solutions for the irradiance standard deviation is less than 10%. These differences in the choice of C are explained by the different methods of evaluating the functions K(z) and R(z). In Ref. 18, we limited ourselves to real and purely empirical expressions; in Ref. 20, we used asymptotic formulas only; but, here, we calculate K(z) and R(z) from the full integral eqs. 47-48.

$$\frac{i}{2k}\left[\langle a^*\nabla^2 a\rangle - \langle a\nabla^2 a^*\rangle\right] \simeq \frac{\Theta^2 z}{2}\,\frac{F}{(F-z)}\,\nabla^2\langle aa^*\rangle\ , \qquad [53]$$

where Θ is the diffractional far-field half-angle beam divergence. For a Gaussian beam with an irradiance e-folding radius w_o, $\Theta = 1/kw_o$.

4.0 COMPARISON OF SOLUTIONS WITH DATA

After substitution of eqs. 22-25, 52 and 53 for the higher order moments in eqs. 10-12, we obtain a closed set of partial differential equations for <A>, <aa> and <aa*>. In nondimensional form, these equations are

$$\left(\frac{\partial}{\partial\eta} + \frac{\rho}{\eta-f}\,\frac{\partial}{\partial\rho}\right)\langle A\rangle - \frac{ib}{2}\nabla_\rho^2\langle A\rangle - bR(\eta)\nabla_\rho^2\langle A\rangle = -\frac{\langle A\rangle}{(\eta-f)} - \frac{1}{2}K(\eta)\langle A\rangle, \qquad [54]$$

$$\left(\frac{\partial}{\partial\eta} + \frac{\rho}{\eta-f}\,\frac{\partial}{\partial\rho}\right)\langle aa\rangle - \frac{ib}{4}\nabla_\rho^2\langle aa\rangle - \frac{b}{2}R(\eta)\nabla_\rho^2\langle aa\rangle + iT(\eta)\langle aa\rangle$$

$$= -\frac{2\langle aa\rangle}{(\eta-f)} + K(\eta)\langle A\rangle\langle A\rangle + 2b\,R(\eta)\,\underset{\sim}{\nabla}\langle A\rangle\cdot\underset{\sim}{\nabla}_\rho\langle A\rangle\ , \qquad [55]$$

$$\left(\frac{\partial}{\partial\eta} + \frac{\rho}{\eta-f}\,\frac{\partial}{\partial\rho}\right)\langle aa^*\rangle - \frac{b^2 f}{(f-\eta)}\,\frac{\eta}{2}\,\nabla_\rho^2\langle aa^*\rangle - \frac{b}{2}\,\mathrm{Real}[R(\eta)]\nabla_\rho^2\langle aa^*\rangle$$

$$= -\frac{2\langle aa^*\rangle}{(\eta-f)} + \mathrm{Real}[K(\eta)]\langle A\rangle\langle A\rangle^* + 2b\,\mathrm{Real}[R(\eta)]\underset{\sim}{\nabla}_\rho\langle A\rangle\cdot\underset{\sim}{\nabla}_\rho\langle A\rangle^*, \qquad [56]$$

where η and ρ are nondimensional variables

$$\eta = z/z_A \text{ and } \rho = r/w_o , \qquad [57a,b]$$

and b and f, similarity parameters

$$b = z_a/kw_o^2 \text{ and } f = F/z_A . \qquad [58a,b]$$

The length scales w_o and z_A are respectively the representative radius of the unperturbed laser beam and the fading distance of the average amplitude given by

$$z_A = 1/C_n^{12/11} \, k^{7/11} , \qquad [59]$$

Finally, the proportionality functions are

$$K(\eta) = \frac{3.24}{\eta_o^{7/6}} \int_o^{\eta} dy \int_o^{y} dx \; \frac{(f-x)^2 \, G(\gamma)}{(f-\eta)^2 \, (f+\eta-2y)} , \qquad [60]$$

$$R(\eta) = \frac{2.43}{\eta_o^{1/6}} \int_o^{\eta} dy \int_o^{y} dx \; \frac{(f-x)^2 H(\gamma)}{(f-\eta)(f+\eta-2y)} , \qquad [61]$$

$$T(\eta) = \begin{cases} C \dfrac{(f-\eta/2)}{(f-\eta)} \dfrac{1}{\eta} \; ; & \eta \leq 1 \; , \\ \\ C \dfrac{(f-\eta/2)}{(f-\eta)} \eta \; ; & \eta > 1 \; , \end{cases} \qquad [62]$$

with

$$\gamma = \frac{\eta_o}{2(\eta-y)} \frac{(f+\eta-2y)\ (f-y)}{(f-x)^2} \; , \qquad [63]$$

which gives rise to a third similarity parameter

$$\eta_o = k\, \ell_1^2 / z_A \; . \qquad [64]$$

However, for $\eta >> \eta_o$, the solutions become virtually independent of η_o.

Equations 54-56 form a closed set of partial differential equations, in three-dimensional space only, for the solution of the statistical moments <A>, <aa> and <aa*>. General solutions to these equations can be worked out in terms of Green's functions but this leads to complicated multiple integrals that are very troublesome and lengthy to evaluate. We find it much more convenient to solve the finite difference version of eqs. 54-56. This approach is straightforward, involves no particular difficulty except in the near vicinity of $\eta = f$, and is applicable to arbitrary beam profiles.

The quantities of interest are the average irradiance and the irradiance variance. The average irradiance is defined by

$$\langle I \rangle = \langle A \rangle \langle A \rangle^* + \langle aa^* \rangle \ , \qquad [65]$$

and the irradiance variance by

$$\sigma_I^2 = \langle (I - \langle I \rangle)^2 \rangle \ . \qquad [66]$$

In terms of amplitude moments, we have

$$\begin{aligned} \sigma_I^2 = {} & \langle aa^*aa^* \rangle - \langle aa^* \rangle^2 + 2\langle A \rangle \langle aa^*a^* \rangle \\ & + 2\langle A \rangle^* \langle aaa^* \rangle + 2\langle A \rangle \langle A \rangle^* \langle aa^* \rangle + \langle A \rangle \langle A \rangle \langle aa \rangle^* \\ & + \langle A \rangle^* \langle A \rangle^* \langle aa \rangle \ . \end{aligned} \qquad [67]$$

Therefore, the irradiance variance depends on statistical moments of orders three and four. Instead of trying to derive a closed set of equations for these higher order moments, we prefer, as a first and simpler attempt of solution, to make a hypothesis regarding the probability distribution of the complex-amplitude fluctuations. We have shown in Refs. 22 and 23 that the hypothesis of normal distribution for the complex amplitude $a(z,r)$ constitutes a consistent approximation over the complete propagation range. The assumption of normal statistics for $a(z,r)$ gives

$$\langle a^*a^*a \rangle = \langle aaa^* \rangle = 0 \ , \qquad [68]$$

$$\langle aa^*aa^* \rangle = 2\langle aa^* \rangle^2 + \langle aa \rangle \langle aa \rangle^* . \qquad [69]$$

Hence, eq. 67 becomes

$$\sigma_I^2 = \langle aa^* \rangle^2 + \langle aa \rangle \langle aa \rangle^* + 2\langle A \rangle \langle A \rangle^* \langle aa^* \rangle + \langle A \rangle \langle A \rangle \langle aa \rangle^* + \langle A \rangle^* \langle A \rangle^* \langle aa \rangle . \qquad [70]$$

Therefore, both the average irradiance and the irradiance variance can be calculated from the solutions of eqs. 54-56. It is noteworthy that the implications of normal statistics for a(z,r) are explicitly and completely specified by eqs. 68 and 69. Most importantly, this hypothesis was not needed to derive the closure relations which form the basis of our model.

To verify our model, a laboratory experiment was designed which allows complete control over the turbulence parameters (Ref. 24). In short, the refractive-index turbulences are produced by creating an unstable vertical temperature gradient in a tank filled with water. This is simply done by heating the water at the bottom of the tank and cooling it at the top. The tank is 1.5 m long, 0.6 m deep and 0.4 m wide. The propagation path is increased by folding the beam lengthwise. Typically, the index structure constant C_n is $10^{-4} m^{-1/3}$.

Figures 5 and 6 show the measured normalized average beam radius w/w_o plotted versus propagation distance for collimated ($f = \infty$) Gaussian beams with w_o equal to 6.0 mm (b=0.0016) and 3.0 mm (b=0.0064) respectively. The data were taken by slowly traversing a point detector across the beam through its center. The radius w was calculated from the measured average irradiance profile $\langle I(r) \rangle$ according to

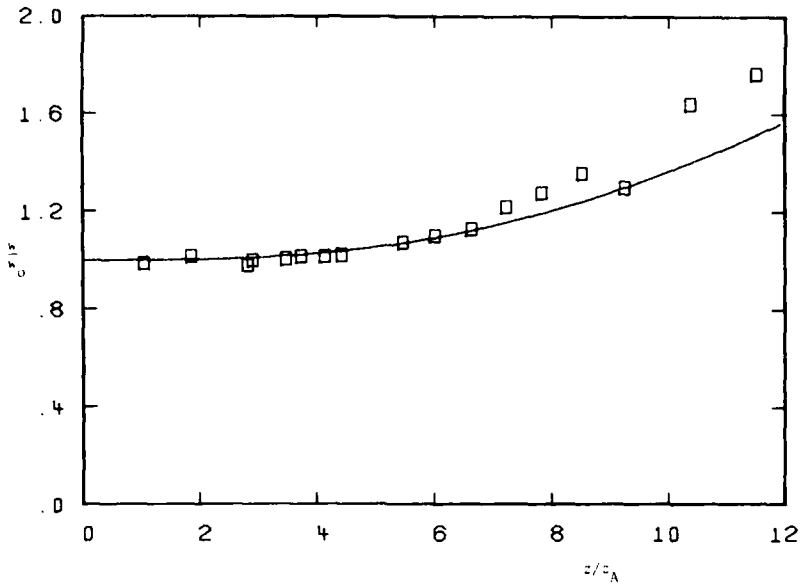

FIGURE 5 - Normalized beam radius plotted versus normalized propagation distance; b = 0.0016, f = ∞, η_o = 7.0. □ : data measured in laboratory turbulence. ——— : finite-difference solution of eqs. 54 and 56.

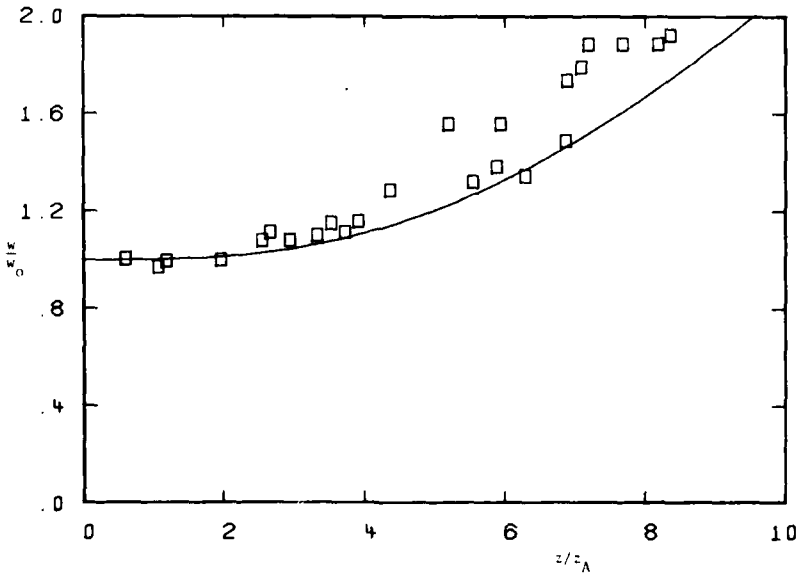

FIGURE 6 - Normalized beam radius plotted versus normalized propagation distance; b = 0.0064, f = ∞, η_o = 7.0. □ : data measured in laboratory turbulence. ———: finite-difference solution of eqs. 54 and 56.

$$w^2 = \int_0^\infty r^3 \langle I(r)\rangle dr \Big/ \int_0^\infty r \langle I(r)\rangle \, dr. \qquad [71]$$

The solid curves represent the theoretical solutions calculated from eqs. 54 and 56. The predicted beam spread is smaller than the measured spread by about 10%. However, the experimental calculation of the beam radius becomes quite sensitive, with increasing radius, to errors in the measured irradiance as indicated by the presence of r to the third power in the integral of the numerator of eq. 71. Since irradiance errors at low level, such as in the wings of the beam, are generally toward higher values, and overestimation of w^2 appears likely. Therefore, we conclude that the turbulence-induced beam spread is satisfactorily predicted by our model. In particular, the influence of the similarity parameter $b = z_A/kw_o^2$ is well verified.

Figures 7 and 8 show similar results for beams focused at f = 3.13 and f = 4.41 respectively. The data were measured from exposed photographs of the beam. The images were digitized and the radii calculated with the formula

$$w^2 = \iint_{-\infty}^{\infty} dxdy(x^2 + y^2) \langle I(x,y)\rangle \Big/ \iint_{-\infty}^{\infty} dxdy \langle I(x,y)\rangle \, . \qquad [72]$$

In this case, the agreement between the data and the predictions of our model is excellent. The average beam radius passes through a minimum which is considerably greater than the diffraction limit value equal to (bf) and this occurs at a propagation distance appreciably shorter than the focal length f. The magnitude of this effect and its dependence on the parameter f are well predicted by our model as illustrated in Figs. 7-8.

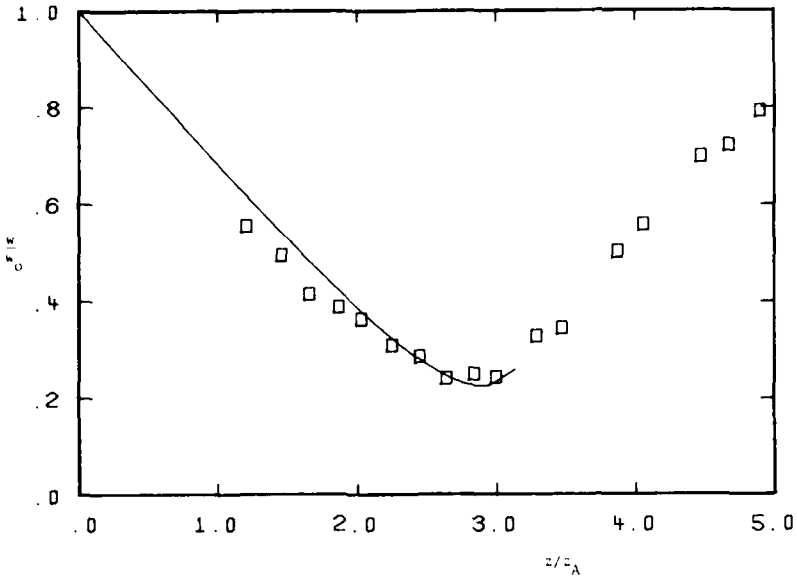

FIGURE 7 - Normalized beam radius plotted versus normalized propagation distance; $f = 3.13$, $b = 0.0023$, $\eta_o = 8.5$. □ : data measured in laboratory turbulence. ————: finite-difference solution of eqs. 54 and 56.

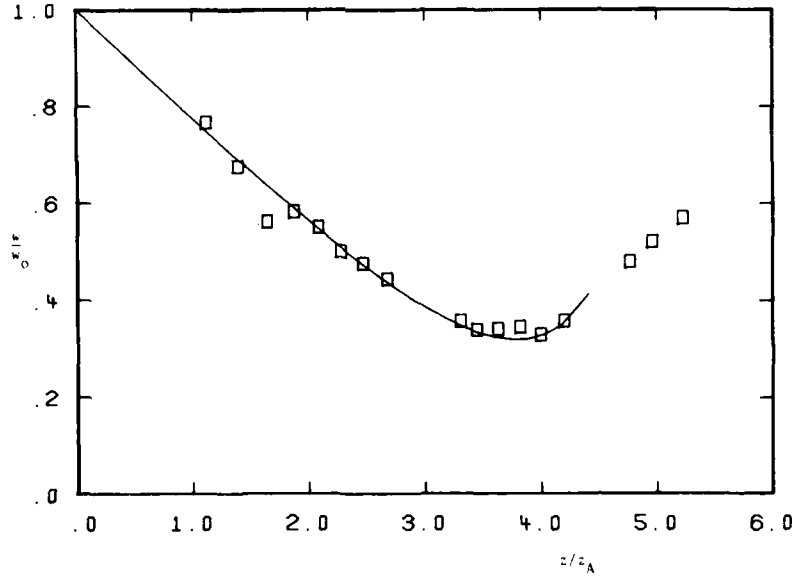

FIGURE 8 - Normalized beam radius plotted versus normalized propagation distance; $f = 4.41$, $b = 0.0021$, $\eta_o = 8.5$. □ : data measured in laboratory turbulence. ————: finite-difference solution of eqs. 54 and 56.

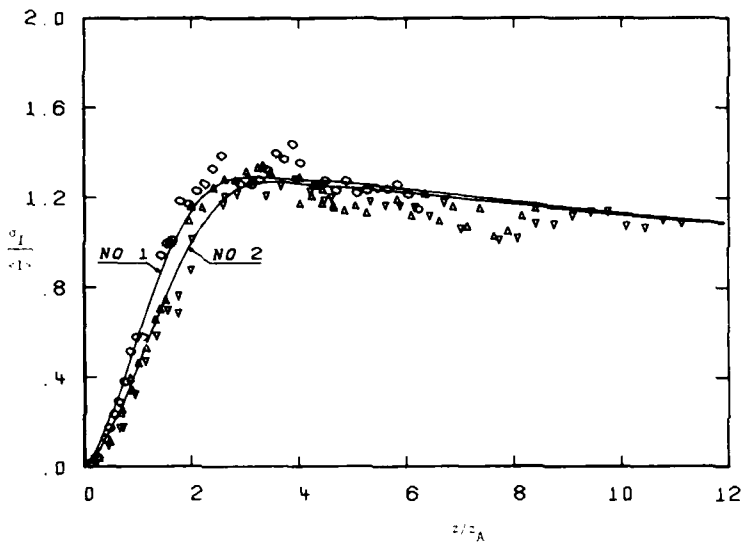

FIGURE 9 - Normalized irradiance standard deviation plotted versus normalized propagation distance. Data measured in laboratory turbulence on the axis of a 25-mm diameter collimated ($f = \infty$) beam. O: $\eta_o = 4.0$, $b = 0.0020$; Δ : $\eta_o = 5.3$, $b = 0.0015$; ∇ : $\eta_o = 7.0$, $b = 0.0011$. ————: finite-difference solution of eqs. 54 - 56, curve No 1 for $\eta_o = 4.0$, $b = 0.0020$ and curve No 2 for $\eta_o = 7.0$, $b = 0.0011$.

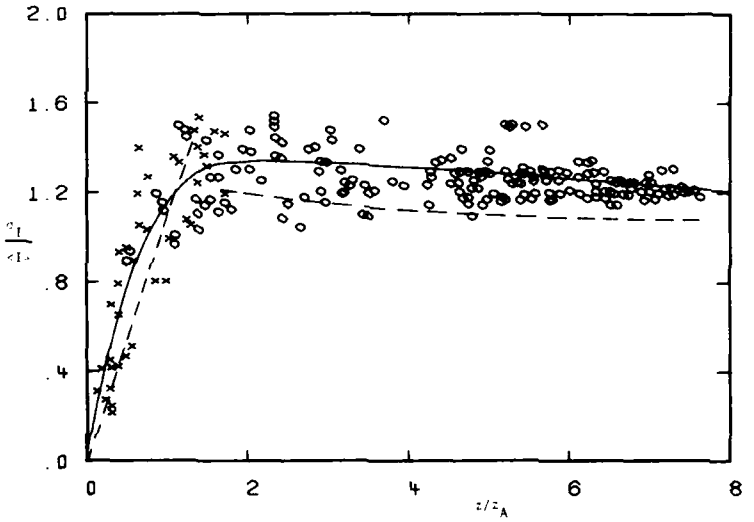

FIGURE 10 - Normalized irradiance standard deviation versus normalized propagation distance. Data measured in the atmosphere and reprinted from Fig. 19 of Ref. 7. ————: finite-difference solution of eqs. 54-56 for plane waves ($f = \infty$, $b = 0$). ---: asymptotic solutions derived in Ref. 7.

Figure 9 compares the irradiance standard-deviation data measured on the axis of collimated beams with the prediction of our model. These results served to determine the empirical constant C of eqs. 52 and 62. To verify that C is universal, the atmospheric data of Fig. 19 of Ref. 7 are plotted in Fig. 10 and compared with our plane-wave solution. The agreement is excellent. Therefore, the results of Figs 9-10 show that our model works very well under experimental conditions that are as far apart as can be expected in practice. Indeed, the propagation distances and the turbulence-strength parameters C_n's differ by more than two orders of magnitude. Therefore, the empirical constant C can in fact be considered universal with good accuracy.

For comparison purposes, we have shown in Fig. 10 the asymptotic solutions derived in Ref. 7 which are representative of the present state of the art. We therefore see that our solutions agree much more closely with data, particularly with regard to the slow return of the data to the asymptotic saturation level of unity.

5.0 SIMPLIFIED SOLUTIONS

Although eqs. 54-56 together with the constitutive eqs. 60-62 are easily solved by numerical techniques, it is useful to consider situations where approximate analytic solutions can be worked out. Despite the necessary restrictive conditions under which these solutions apply, the analytic expressions give helpful information regarding the influence of the various parameters and the magnitude of the turbulence-induced phenomena. One such simplification is afforded by the study of untruncated Gaussian beams.

5.1 Average irradiance

For an initially Gaussian beam with the normalized average amplitude given by

$$\langle A \rangle_{\eta=0} = e^{-\rho^2/2} , \qquad [73]$$

it is straightforward to show that the solution of eq. 54 is

$$\langle A \rangle = g(\eta)\ e^{-\rho^2/2\sigma^2(\eta)} , \qquad [74]$$

where

$$g(\eta) = \frac{f-\eta}{f\sigma^2(\eta)}\ \exp\left\{-\frac{1}{2}\int_0^\eta K(\zeta)d\zeta\right\}, \qquad [75]$$

$$\sigma^2(\eta) = \frac{(f-\eta)^2}{f^2} - bi\,\frac{\eta(\eta-f)}{f} + 2b\int_0^\eta \frac{(f-\eta)^2}{(f-\zeta)^2}\,R(\zeta)d\zeta . \qquad [76]$$

If turbulence-induced beam spreading dominates over diffraction-spreading and if the condition

$$[\mathrm{Imag}(\sigma^2)]^2/[\mathrm{Real}(\sigma^2)]^2 \ll 1 \qquad [77]$$

is satisfied, which occurs in most applications, eq. 56 for $\langle aa^* \rangle$ can be solved analytically and we find for the average irradiance

$$\langle I \rangle = \{1 - h(\eta)[1 - \rho^2/w^2(\eta)]\} \frac{e^{-\rho^2/w^2(\eta)}}{w^2(\eta)} , \quad [78]$$

where

$$h(\eta) = \frac{2b}{w^2(\eta)} \frac{(f-\eta)^2}{f^2} \int_0^\eta \frac{d\zeta}{w^2(\zeta)} \text{Real}[R(\zeta)] \exp\{-\int_0^\zeta \text{Real}[K(\xi)]d\xi\}, \quad [79]$$

$$w^2(\eta) = \frac{(f-\eta)^2}{f^2} + 2b\int_0^\eta \frac{(f-\eta)^2}{(f-\zeta)^2} \text{Real}\ [R(\zeta)]d\zeta. \quad [80]$$

Equation 78 shows that the turbulence-spread Gaussian beam does not truly conserve its Gaussian shape; too much irradiance is scattered in the wings as inferred by the ρ^2-term multiplying the exponential function. *However, in many practical applications, the similarity* parameter b is much smaller than unity and the function $h(\eta)$ can be neglected in eq. 78 to give

$$\langle I \rangle \simeq \frac{e^{-\rho^2/w^2(\eta)}}{w^2(\eta)} . \quad [81]$$

An important simplification can be made to the proportionality function $R(\eta)$ if we assumed that $\eta_o << 1$. This condition is almost always satisfied for atmospheric propagation of optical and infrared beams. For example, at $\lambda = 0.63$ μm, η_o is equal to about 10^{-3} for very strong turbulence ($C_n = 10^{-6} m^{-1/3}$) and smaller for weaker turbulence. *Under this condition*, the asymptotic formula

$$\lim_{\gamma \to 0} H(\gamma) = \frac{5}{6} \Gamma(5/6)(-i\gamma)^{-1/6} \qquad [82]$$

can be substituted for $H(\gamma)$ in eq. 61 and we find

$$\text{Real}[R(\eta)] = 0.738 \int_0^{\eta} dy \frac{\left[f^{8/3} - (f-y)^{8/3}\right](f-y)^{1/6}}{(f-\eta)(f+\eta-2y)^{5/6}(\eta-y)^{1/6}} \quad . \qquad [83]$$

This integral cannot be worked out in terms of elementary transcendental functions. However, for the following discussion, it suffices to consider collimated beams, i.e. $f = \infty$, which yields

$$\text{Real}[R(\eta)] = 1.288\ \eta^{11/6} \quad . \qquad [84]$$

Upon substituting eq. 84 for $R(\eta)$ in eq. 80, we therefore have for collimated beams

$$w^2(\eta) = 1 + 0.909\ b\ \eta^{17/6} \quad . \qquad [85]$$

Thus, the turbulence-induced beam spread predicted by our model and valid under the conditions [77] and $\eta_o << 1$ is given, in dimensional variables, by

$$p^2(z) = w_o^2 + 0.909\ k^{1/6}\ \frac{C_n^2}{n_o^2}\ z^{17/6}. \qquad [86]$$

The beam-spread expression most often used in the literature is that derived by Brown (Ref. 25) and Yura (Ref. 26). It is based on the reasoning that the turbulence-induced beam spread can be no smaller than that produced by a transmitter with an aperture equal to the coherence diameter $\rho_o = (0.545\ k^2 z C_n^2/n_o^2)^{-3/5}$. The formula given by Yura is

$$p_Y^2 = w_o^2 + 1.93\ k^{2/5}\ z^{16/5}\ \ (C_n/n_o)^{12/5}\ . \qquad [87]$$

We note that both ours and Brown's or Yura's expressions depend on the same three parameters k, C_n/n_o and z. In particular, they are independent of beam or aperture size which confirms the experimental observation that turbulence spreading cannot be corrected by increasing the transmitter aperture. However, the functional dependence on k, C_n/n_o and z is slightly different in both cases. Our expression predicts a weaker dependence on all three parameters.

Systematic turbulence beam-spread measurements were performed by Dowling and Livingston (Ref. 27). For total far-field turbulence-induced beam divergence, they proposed the following empirical regression formula

$$\Theta^2_{DL} = 2.9 \times 10^{-6}\ k^{1/3}\ z\ (C_n/n_o)^{6/5}. \qquad [88]$$

Table I compares the predictions obtained from eqs. 86 and 87, i.e.

$$\Theta^2_B = 7.27\ k^{1/6}\ Z^{5/6}\ (C_n/n_o)^2\ , \qquad [89]$$

$$\Theta^2_Y = 15.44\ k^{2/5}\ Z^{6/5}\ (C_n/n_o)^{12/5}\ , \qquad [90]$$

with those of eq. 88 for the upper, middle and lower C_n values reported in Ref. 27. Our model gives a somewhat more consistent fit to the empirical formula. The discrepancies come mainly from our stronger C_n dependence compared with that of eq. 88. However, it is shown in the same Ref. 27 that the optical data (λ = 0.63 μm) are also well fitted by a linear regression against $C_n^2 z$ which has the same C_n power as our model and only a difference of 1/6 in the power of propagation distance. Therefore, the beam-spread formula derived from the propagation model of this report appears to be more precise than the generally used formula of Brown and Yura, although more data with greater parameter ranges are still needed.

TABLE I

Comparison of the theoretical beam-spread formula of this report (Θ_B, eq. 89) and that of Ref. 26 (Θ_Y, eq. 90) with the empirical regression formula (Θ_{DL}, eq. 88) proposed in Ref. 27. The propagation distance z is 1750 m and the C_n-values correspond to the upper, middle and lower turbulence levels reported in Ref. 27.

	λ = 0.63 μm			λ = 10.6 μm		
C_n ($m^{-1/3}$)	Θ_{DL} (μrad)	Θ_B (μrad)	Θ_Y (μrad)	Θ_{DL} (μrad)	Θ_B (μrad)	Θ_Y (μrad)
8×10^{-7}	229	185	420	143	147	239
5×10^{-7}	173	116	239	108	92	136
1×10^{-7}	66	23	35	41	18	20

5.2 Irradiance variance

Under the same simplifying assumptions as used to derive eq. 81 for the average irradiance, it is easy to show from eqs. 54-56 and 70 that the corresponding irradiance variance profile has the form

$$\sigma_I^2 = F(\eta)\, e^{-\rho^2/w^2(\eta)}, \qquad [91]$$

where $F(\eta)$ contains integrals that cannot be reduced to elementary transcendental functions. However, the important conclusion from eqs. 91 and 81 is that the normalized irradiance variance, $\sigma_I^2/\langle I\rangle^2$, is independent of lateral position across the beam but varies with propagation distance only. Within the experimental scatter, this is well verified in our simulated turbulent medium.

For plane waves, the function $F(\eta)$ of eq. 91 reduces to a simple asymptotic formula valid for $\eta < 1$. The solution for the irradiance variance is thus

$$\frac{\sigma_I^2}{\langle I\rangle^2} = 2.76\, k^{7/6}\, Z^{11/6}\, C_n^2/n_o^2 . \qquad [92]$$

Except for the numerical constant, this expression is identical with the perturbation result given by Tatarskii (Ref. 2), i.e.

$$\left[\frac{\sigma_I^2}{\langle I\rangle^2}\right]_T = 1.23\, k^{7/6}\, Z^{11/6}\, C_n^2/n_o^2 . \qquad [93]$$

Equation 92 corresponds to the weak-scintillation asymptote of the plane-wave solution shown as the solid curve in Fig. 10 while Tatarskii's solution, eq. 93, is plotted as the broken line through the origin in the same figure. We thus see that either solution is equally justifiable on the basis of the low-scintillation data of Fig. 10. Therefore, we conclude that the propagation model proposed in this report is in good agreement with the results of the classical perturbation theory.

6.0 CONCLUSION

The mathematical model of laser-beam propagation in turbulence originally developed in Refs. 18 and 20 was extended to include focalization. The model is in the form of a closed set of three simultaneous second-order partial differential equations for the complex-amplitude moments of order one and two. The important and novel characteristic of these equations is that they are numerically tractable and uniformly valid for arbitrary scintillation levels.

The solutions were calculated with a finite-difference algorithm. The agreement with measured average irradiance profiles for collimated and focused beams is excellent. The predicted irradiance variance clearly shows supersaturation and is well verified by data ranging from the perturbation to the asymptotic saturation regimes. An analytic expression for the turbulence-induced spreading of Gaussian beams was derived. Comparison with data showed that it is somewhat more precise than the commonly used formula based on the concept of the coherence diameter ρ_o. Finally, the irradiance variance solution in the weak-scintillation limit agrees with the classical results of the perturbation theory.

Extension of the model to media with varying and/or nonlinear average refractive index is straightforward. In particular, the thermal-blooming effect in the presence of turbulence could be calculated with only a small increase in computation time compared with the non-turbulent case. The model could also be used to simulate the propagation of beams corrected by adaptive systems. The principal requirement would be to rederive the solutions for the functions $K(z)$ and $R(z)$ with the proper boundary conditions on the covariance of the angle-of-arrival.

7.0 ACKNOWLEDGMENTS

We are pleased to acknowledge the able technical assistance of P. Guay for data reduction and handling, and A. Perreault and R. Rochette for setting up the simulation facility and participating in data acquisition. The photographs of the beam were digitized using an automated system developed by J. Boulter whose assistance was greatly appreciated. We would also like to thank M. Gravel for helpful discussions.

8.0 REFERENCES

1. Tatarskii, V.I., "Wave Propagation in a Turbulent Medium", Dover Publication, New York, 1967.

2. Tatarskii, V.I., "The Effects of the Turbulent Atmosphere on Wave Propagation", National Technical Information Service, U.S. Dept. of Commerce, Springfield, Va., 1971, UNCLASSIFIED

3. De Wolf, D.A., "Saturation of Irradiance Fluctuations Due to Turbulent Atmosphere", J. Opt. Soc. Am., Vol. 58, No. 4, p. 461, 1968.

4. De Wolf, D.A., "Strong Irradiance Fluctuations in Turbulent Air: Plane Waves", J. Opt. Soc. Am., Vol. 63, No. 2, p. 171, 1973.

5. De Wolf, D.A., "Strong Irradiance Fluctuations in Turbulent Air, II. Spherical Waves", J. Opt. Soc. Am., Vol. 63, No. 10, p. 1249, 1973.

6. De Wolf, D.A., "Strong Irradiance Fluctuations in Turbulent Air, III. Diffraction Cutoff", J. Opt. Soc. Am., Vol. 64, No. 3, p. 360, 1974.

7. Prokhorov, A.M., Bunkin, F.V., Gochelashvily, K.S. and Shishov, V.I., "Laser Irradiance Propagation in Turbulent Media", Proc. of the IEEE, Vol. 63, No. 5, p. 790, 1975.

8. Brown, W.P. Jr., "Fourth Moment of a Wave Propagating in a Random Medium", J. Opt. Soc. Am., Vol. 62, No. 8, p. 966, 1972.

9. Beran, J.J. and Whitman, A.M., "Free-Space Propagation of Irradiance Fluctuations and the Fourth-Order Coherence Function", J. Opt. Soc. Am., Vol. 64, No. 12, p. 1636, 1974.

10. Fante, R.F., "Irradiance Scintillation: Comparison of Theory with Experiment", J. Opt. Soc. Am., Vol. 65, No. 5, p. 548, 1975.

11. Whitman, A.M. and Beran, J.J., "Asymptotic Theory of Irradiance Fluctuations in a Beam Propagating in a Random Medium", J. Opt. Soc. Am., Vol. 65, No. 7, p. 765, 1975.

12. Lutomirski, R.F. and Yura, H.T., "Propagation of Finite Optical Beam in an Inhomogeneous Medium", Appl. Opt., Vol. 10, No. 7, p. 1652, 1971.

13. Yura, H.T., Physical Model for Strong Optical Amplitude Fluctuations in a Turbulent Medium", J. Opt. Soc. Am., Vol. 64, No. 1, p. 59, 1974.

14. Clifford, S.F., Ochs, G.R. and Lawrence, R.S., "Saturation of Optical Scintillation by Strong Turbulence", J. Opt. Soc. Am., Vol. 64, No. 2, p. 148, 1974.

15. Banakh, V.A., Krekov, G.M., Mironov, V.L., Khmelevtsov, S.S. and Tsvik, R. Sh., "Focused-Laser-Beam Scintillations in the Turbulent Atmosphere", J. Opt. Soc. Am., Vol. 64, No. 4, p. 516, 1974.

16. Lee, H.M., Elliot, R.A., Holmes, J.F. and Kerr, J.R., "Variance of Irradiance for Saturated Scintillations", J. Opt. Soc. Am., Vol. 66, No. 12, p. 1389, 1976.

17. Dunphy, J.R. and Kerr, J.R., "Turbulence Effects on Target Illumination by Laser Sources: Phenomenological Analysis and Experimental Results", Appl. Opt., Vol. 16, No. 5, p. 1345, 1977.

18. Bissonnette, L.R., "Average Irradiance and Irradiance Variance of Laser Beams in Turbulent Media", DREV R-4104/78, May 1978, UNCLASSIFIED

19. Bradshaw, P., Editor, "Turbulence", Topics in Applied Physics, Vol. 12, Springer-Verlag, New York, 1976.

20. Bissonnette, L.R., "Modelling of Laser Beam Propagation in Atmospheric Turbulence", pp 73-94, Proceedings of the Second International Symposium on Gas-Flow and Chemical Lasers, John F. Wendt editor, Hemisphere Publishing Corporation, Washington, D.C. (1979).

21. Abramowitz, M. and Stegun, I.A., "Handbook of Mathematical Functions", Dover Publications, New York, 1965.

22. Bissonnette, L.R., "Probability Distribution and Asymptotic Variance of Strong Irradiance Fluctuations of Optical Waves in Turbulent Media", DREV R-4042/75, October 1975. UNCLASSIFIED; "Log-Normal Probability Distribution of Strong Irradiance Fluctuations: an Asymptotic Analysis", AGARD Conference Proceedings No. 183 on Optical Propagation in the Atmosphere (Defence Scientific Information Service, Ottawa), 1975. UNCLASSIFIED.

23. Bissonnette, L.R. and Wizinowich, P.L., "Irradiance Probability Distribution in Saturation Regime of Optical Waves Propagating in Turbulence", DREV R-4114/78, August 1978, UNCLASSIFIED; "Probability Distribution of Turbulent Irradiance in a Saturation Regime", Appl. Opt., Vol. 18, No. 10, pp. 1590, 1979.

24. Bissonnette, L.R., "Laboratory Simulation of Atmospheric Turbulence for Optical Propagation Studies", DREV Report 4075/77, August 1977, UNCLASSIFIED; "Atmospheric Scintillation of Optical and Infrared Waves: a Laboratory Simulation", Appl. Opt., Vol. 16, No. 8, p. 2242, 1977.

25. Brown, W.P. Jr, "Second Moment of a Wave Propagating in a Random Medium", J. Opt. Soc. Am., Vol. 61, No. 8, p. 1051, August 71.

26. Yura, H.T., "Atmospheric Turbulence Induced Laser Beam Spread", Appl. Opt., Vol. 10, No. 12, p. 2771, December 1971.

27. Dowling, J.A. and Livingston, P.M., "Behavior of Focused Beams in Atmospheric Turbulence: Measurements and Comments on the Theory", J. Opt. Soc. Am., Vol. 63, No. 7, p. 846, July 1973.

CRDV R-4178/80 (NON CLASSIFIE)

Bureau - Recherche et Développement, MDN, Canada.
CRDV, C.P. 880, Courcelette, Qué. GOA 1RO

"Faisceaux laser focalisés en milieux turbulents."
par L.R. Bissonnette

On dérive un système fermé de trois équations simultanées aux dérivées partielles pour résoudre l'intensité moyenne et la variance de l'intensité de faisceaux laser focalisés en propageant dans un milieu turbulent. Ces équations sont uniformément valides à tous les niveaux de scintillation. Des exemples de solutions calculées numériquement sont en excellent accord avec des mesures obtenues dans l'atmosphère et en laboratoire. On dérive de ces équations une expression analytique de la diffusion par la turbulence et on démontre que celle-ci est plus précise que la formule généralement employée et tirée du concept du diamètre de cohérence ρ_0. Dans la limite des scintillations faibles, la solution pour la variance de l'intensité recoupe les résultats classiques de la théorie de perturbation. (NC)

CRDV R-4178/80 (NON CLASSIFIE)

Bureau - Recherche et Développement, MDN, Canada.
CRDV, C.P. 880, Courcelette, Qué. GOA 1RO

"Faisceaux laser focalisés en milieux turbulents."
par L.R. Bissonnette

On dérive un système fermé de trois équations simultanées aux dérivées partielles pour résoudre l'intensité moyenne et la variance de l'intensité de faisceaux laser focalisés en propageant dans un milieu turbulent. Ces équations sont uniformément valides à tous les niveaux de scintillation. Des exemples de solutions calculées numériquement sont en excellent accord avec des mesures obtenues dans l'atmosphère et en laboratoire. On dérive de ces équations une expression analytique de la diffusion par la turbulence et on démontre que celle-ci est plus précise que la formule généralement employée et tirée du concept du diamètre de cohérence ρ_0. Dans la limite des scintillations faibles, la solution pour la variance de l'intensité recoupe les résultats classiques de la théorie de perturbation. (NC)

CRDV R-4178/80 (NON CLASSIFIE)

Bureau - Recherche et Développement, MDN, Canada.
CRDV, C.P. 880, Courcelette, Qué. GOA 1RO

"Faisceaux laser focalisés en milieux turbulents."
par L.R. Bissonnette

On dérive un système fermé de trois équations simultanées aux dérivées partielles pour résoudre l'intensité moyenne et la variance de l'intensité de faisceaux laser focalisés en propageant dans un milieu turbulent. Ces équations sont uniformément valides à tous les niveaux de scintillation. Des exemples de solutions calculées numériquement sont en excellent accord avec des mesures obtenues dans l'atmosphère et en laboratoire. On dérive de ces équations une expression analytique de la diffusion par la turbulence et on démontre que celle-ci est plus précise que la formule généralement employée et tirée du concept du diamètre de cohérence ρ_0. Dans la limite des scintillations faibles, la solution pour la variance de l'intensité recoupe les résultats classiques de la théorie de perturbation. (NC)

CRDV R-4178/80 (NON CLASSIFIE)

Bureau - Recherche et Développement, MDN, Canada.
CRDV, C.P. 880, Courcelette, Qué. GOA 1RO

"Faisceaux laser focalisés en milieux turbulents."
par L.R. Bissonnette

On dérive un système fermé de trois équations simultanées aux dérivées partielles pour résoudre l'intensité moyenne et la variance de l'intensité de faisceaux laser focalisés en propageant dans un milieu turbulent. Ces équations sont uniformément valides à tous les niveaux de scintillation. Des exemples de solutions calculées numériquement sont en excellent accord avec des mesures obtenues dans l'atmosphère et en laboratoire. On dérive de ces équations une expression analytique de la diffusion par la turbulence et on démontre que celle-ci est plus précise que la formule généralement employée et tirée du concept du diamètre de cohérence ρ_0. Dans la limite des scintillations faibles, la solution pour la variance de l'intensité recoupe les résultats classiques de la théorie de perturbation. (NC)

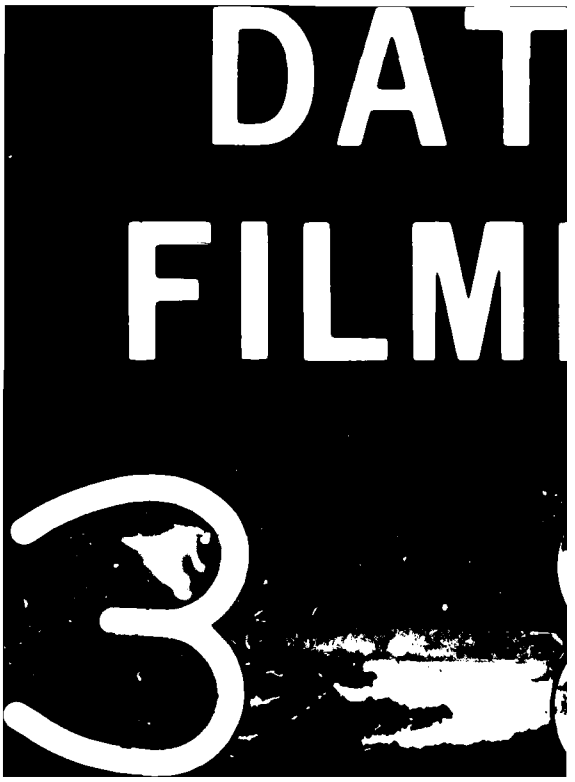
DAT
FILM
3